42nd AIAA/ASME/SAE/ASEE Joint Propulsion Conference & Exhibit
9 - 12 July 2006, Sacramento, California

AIAA 2006-4823

An Optical Diagnostic for Xenon Hall Thrusters Including Metastable Contributions

Jason D. Sommerville* and Lyon B. King.†
Michigan Technological University, Houghton, MI 49931, USA

A laboratory Hall-effect thruster plume has been studied using optical emission spectroscopy. The emissions are compared to a collisional-radiative model which incorporates emission enhancement from fast moving ions and metastable states. Spatially resolved electron temperatures have been measured using the model via imaging spectroscopy and the Abel inversion. The results show a flat temperature distribution for the region of the plume investigated. By comparing the data to two forms of the model, one which includes the fast ion contributions and one which does not, we show that it is possible to determine the beam divergence optically.

Nomenclature

d	=	Distance from exit plane of the thruster
e	=	Electronic charge
E_e	=	Electron energy
I_λ	=	Modeled line intensity
k	=	Boltzmann constant
$\dot{m}$	=	HET mass flow rate
m_e	=	Electon mass
m_i	=	Ion mass
M_λ	=	Metastable enhancement factor
n	=	Ionization level
n_0	=	Neutral atom density
n_e	=	Electron density
q	=	Particle charge number
r	=	Radial distance from thrust axis
$r_{\max}$	=	Approximate radial beam extent
T_e	=	Electron temperature
y	=	Cartesian distance from thrust axis
α	=	Ionization fraction
θ	=	Divergence half-angle
λ	=	Wavelength
σ_{e_λ}	=	Electron impact induced emission cross section
σ_{n_λ}	=	n^{th} level ion impact induced emission cross section

I. Introduction

HALL-effect thrusters (HETs) are fuel-efficient alternatives to chemical propulsion for many earth-orbiting and deep space applications. Nearly all modern HETs use xenon as their propellant. While work has been done utilizing other propellants such as bismuth,[1] it is likely that xenon will remain the propellant of choice for many years.

The ability to study the operating conditions of a xenon-fueled HET using only the radiation emitted from the plasma would be beneficial to HET research. Most importantly, such a diagnostic would be completely non-

* Graduate Research Assistant, Department of Mechanical Engineering-Engineering Mechanics, 815 R. L. Smith Bldg, Houghton, MI 49931, AIAA Student Member.
† Associate Professor, Department of Mechanical Engineering-Engineering Mechanics, 815 R. L. Smith Bldg, Houghton, MI 49931, AIAA Member.

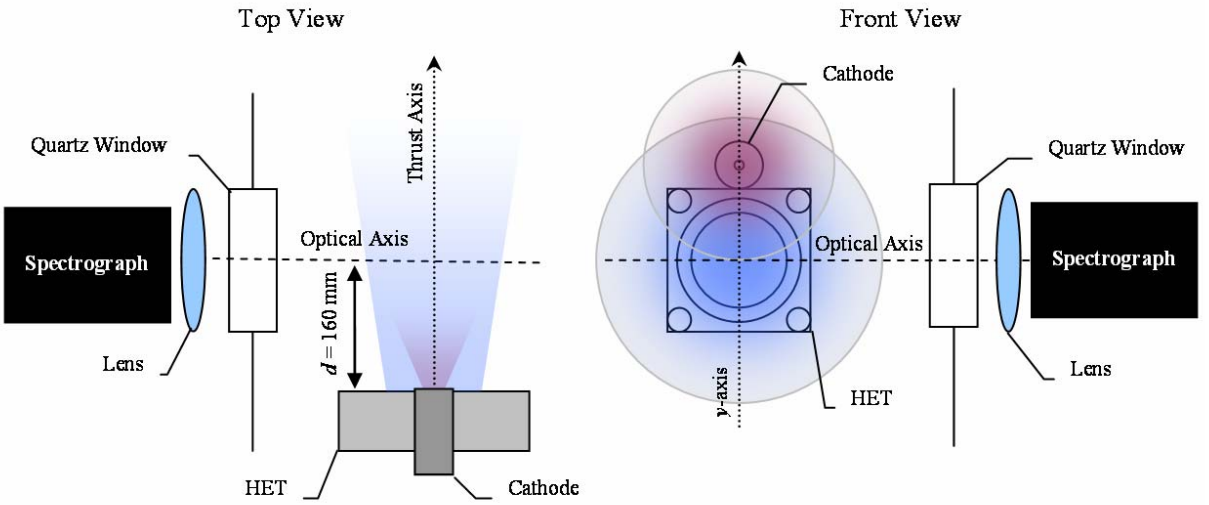

Figure 1. Schematic diagram of the HET emission experiment

invasive, guaranteeing that plasma conditions have not been disturbed by the measurement. In addition, hot regions of plasma, as present in the discharge chamber of a HET, are difficult to study using electrostatic probe techniques. Probe ablation and plasma disturbances induced by rapidly moving probes introduce errors in the measurements.

The spectral content of the radiation carries with it important information about the conditions of the plasma from which the radiation was emitted. Optical emission spectroscopy (OES) is the process of decoding this information and determining the plasma parameters such as electron temperature and density. This technique requires an emission model for the plasma which relates the expected emissions at various spectral lines to specific plasma conditions. If the model describes the plasma sufficiently well, the model outputs may be fit to actual plasma data, thereby determining the parameters of the plasma. Several attempts have been made to measure electron temperature,[2,3] electron energy distribution,[4] and neutral xenon density[5] using such methods.

To date, most researchers have assumed a coronal equilibrium model.[6] However, it has been found that this model falls short in accurately describing the complexities of HET plasmas.[7,8] Here we apply a more complex, collisional-radiative model (CRM) developed by Karabadzhak, Chiu and Dressler (KCD), which incorporates stepwise electron excitation through metastable states and heavy particle collisions,[9] both of which have been proposed to be an important source of HET radiation.[2,7,8,10]

II. Hall Effect Thruster Emission Experiment

In order to improve OES on xenon-fueled HETs, we are investigating the accuracy of the KCD model. This paper reports on the application of the model to the emissions of the plume of a laboratory 2-kW HET similar to an Aerojet BPT-2000.[11] The experiment is similar to an experiment already reported by KCD on an anode layer thruster (TAL).[9] In addition to investigating a different thruster, we have used a spectrographic imaging technique to acquire multiple spectra simultaneously. The main goals of this experiment were to develop the diagnostic technique, from data acquisition through data reduction via the KCD model, and to provide further validation for the model. This is the first of such work performed in the Isp Laboratory at Michigan Tech.

A. Experimental Setup

The thruster was run at several operating conditions, but all of the data discussed in this paper were acquired while the thruster was running at its nominal operating parameters of $V = 300$ V and $\dot{m} = 5$ mg/s. With these parameters, the thruster drew 5.1 A of current, resulting in operation at 1.53 kW of power. Thruster operation was stable, but the cathode appeared to be leaking an excessive amount of gas, as judged from an anomalous plasma glow surrounding the thruster which was brightest near the back of the cathode.

The emissions passed through a quartz window, and were collected by a 40-mm-focal-length lens and imaged on the entrance slit of Czerny-Turner spectrograph (see Figure 1) with an attached CCD detector. The optical axis was located 160 mm downstream of the thruster exit plane. By using the CCD in imaging mode, we collected one spatial and one spectral dimension of data. In the setup, the spatial dimension corresponds to the *y*-axis of the plume. A

50-mm-focal-length cylindrical lens was placed inside the spectrograph between the focusing mirror and the CCD detector to correct for the astigmatism that is inherent in the Czerny-Turner design.[12] Figure 2 shows the image of the spatial calibration target placed on the detector axis as viewed by the CCD detector through the spectrograph with the grating at zero-order and the slit removed. The ellipsoid frame of the picture is the edge of the quartz window. The bright smear in the upper left is a reflection off of a metal clip that held the target. The curvature distortion, or smile, is also inherent in the spectrograph configuration, but it is unimportant because it is in the spectral dimension and can be corrected through calibration. The focus distortion is the more important problem and limits the spatial resolution of the spectrograph. It is clear that this method is not as ideal as using a proper imaging spectrograph. None-the-less the resolution was sufficient to allow for at least 32 pixels of spatial resolution across the entire detector.

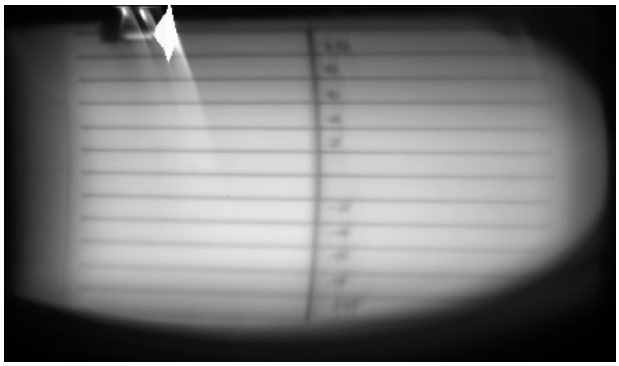

Figure 2. Spatial calibration target as viewed by the spectrograph

The entire spectral region of interest cannot be captured in one exposure by the spectrograph. Spectra taken at multiple grating angles must be combined. At each grating angle, an optimal exposure time was determined such that the signal made close to full use of the range of the A/D converter on the detector without saturating it. These exposure times varied from 1 millisecond to 4 seconds. It was later determined that the shutter speed was not accurate below 10 milliseconds. The implications of this will be discussed in the next section. Future experiments will use neutral density filters to ensure that bright regions of the spectrum may be acquired with exposure times greater than 10 ms without saturating the detector.

The spectral sensitivity of the system was determined by the use of a halogen-tungsten lamp. The light from this lamp was reflected off of a panel painted with a barium sulfide paint that is a diffuse reflector with an even spectral response over the range from 400 nm to 1000 nm. The panel was placed on the thruster axis and the lamp placed at the edge of the vacuum chamber to achieve spatially even illumination. The 25-mm diameter of the lens was slightly smaller than the ~35-mm width of the CCD detector. Thus, the edge of the lens created an aperture and the entire width of the CCD could not be used. The portions of each spectrum that fell outside the cylindrical lens were discarded.

A cylindrical Langmuir probe was also used to measure the temperature along the optical axis of the spectrograph to provide comparative data. The electron temperatures were extracted via an exponential fit to the portion of the trace between floating potential and the first inflection point at a voltage greater than floating potential.[13]

B. Optical Emission Data

The KCD model relates the line intensities to electron temperature. The intensity of each spectral line is modeled by

$$I_\lambda = n_0 n_e \left[\left\langle \sigma_{e_\lambda} v \right\rangle + \alpha \left\langle \sigma_{1_\lambda} v \right\rangle + \frac{(1-\alpha)}{2} \left\langle \sigma_{2_\lambda} v \right\rangle \right] \left[1 + M_\lambda (T_e, \alpha) \right] \tag{1}$$

where $M_\lambda(T_e,\alpha)$ is the enhancement in the line due to the metastable population, the details of which are presented in the paper by Karabadzhak, et al.[9] The electrons are assumed to have a Maxwellian distribution such that the electron impact excitation rate coefficient is given by

$$\left\langle \sigma_{e_\lambda} v \right\rangle = \int_0^\infty 2E_e \sqrt{\frac{2}{\pi (kT_e)^3 m_e}} \exp\left(-\frac{E_e}{kT_e} \right) \sigma_{e_\lambda}(E_e) dE_e \ , \tag{2}$$

and the ions are assumed to be mono-energetic such that the ion impact excitation rate coefficients are given by

Wavelength (nm)	Upper State	Lower State
788.74	$2p_2$	$1s_2$
823.16	$2p_6$	$1s_5$
828.01	$2p_5$	$1s_5$
834.68	$2p_1$	$1s_2$
841.92	$2p_7$	$1s_5$
881.94	$2p_8$	$1s_5$
904.54	$2p_9$	$1s_5$
916.27	$2p_7$	$1s_4$
979.97	$2p_{10}$	$1s_5$

Table 1. Xenon transitions used in the OES diagnostic.

$$\left\langle \sigma_{n_\lambda} v \right\rangle = \sigma_{n_\lambda}(eV)\sqrt{\frac{neV}{m_i}}\,, \tag{3}$$

for the n^{th} level ion where V is the discharge voltage of the HET and m_i is the ion mass.

These equations may be used to model any of the lines of neutral xenon, but we have chosen to apply a 9-line and a 3-line model. The 9-line model uses all of the transitions listed in Table 1. These transitions originate from the $5p^5 6p$ (2p, Paschen notation) configuration and transition to the $5p^5 6s$ configuration (1s, Paschen notation). We have chosen these lines because they are in a sparsely populated region of the spectrum, making line identification easy, and cross section data for the lines is available.[10,14] The 3-line model uses only the lines uncoupled from metastable states, that is $M_\lambda = 0$. Specifically, these lines are at 788 nm, 828 nm, and 834 nm. The intensities of the 788 nm and the 834 nm lines are relatively small and are thus prone to higher errors. However, because they are not coupled to metastable states, they are free from the approximations currently used to estimate the metastable enhancement factor.

The acquired spectra are calibrated for exposure time, background, and spectral sensitivity using standard techniques. However, the exposure time, t, was determined to be inaccurate for many of the spectral segments covering the transitions of interest. Because the model is based on relative transition intensities, and because there was significant overlap between each of the segments corresponding to different grating angles, correction factors for the exposure times could be deduced by normalizing the overlapping portions of each segment to its adjacent segments. This process introduced approximately 10% error in relative peak height from one segment to the next.

The intensities of the lines of interest were calculated for each track of data and are plotted in Figure 3. Each track is mapped to a physical position using the target image acquired through the spectrograph (Figure 2). The numbers printed on the target are in centimeters. If the plume is assumed to be radially symmetric, then the Abel inversion may be used to convert these line intensities as a function of y to point intensities as function of the radial dimension, r. However, a brief glance at Figure 3 shows that the data is not entirely symmetric. The increased intensities above the thrust axis (positive displacements) are most likely a result of the cathode plume. Because the cathode plume represents a significant departure from radial symmetry, the Abel inversion produces questionable results. We therefore focus on the data below the thrust axis where the emission contributions from the cathode plume are less prevalent.

The Abel inversion algorithm used generates a cubic spline through the data, and then inverts the spline.[15] The Abel inversion requires that the signal vanishes at $r = \infty$, and a discretized version of the inversion generally needs to maintain that requirement by ensuring that the signal is small in the edge data points. However, the signal was not sufficiently small at the edges in this experiment. We believe that there is a significant amount of radiation reflecting off of vacuum chamber surfaces and entering the detector. Future experiments will physically mitigate this problem with non-reflective surfaces used for backdrops. For the present data the signal at -130 mm, a point beyond the main

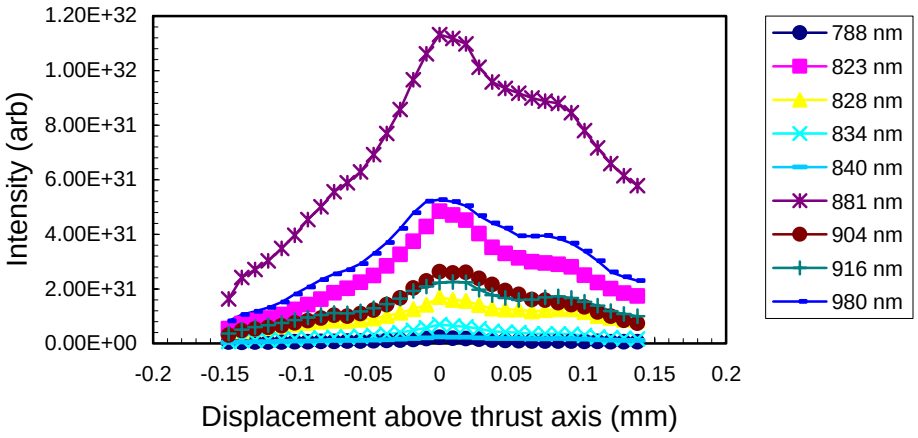

Figure 3. Line intensities from the plume 160 mm downstream of the exit plane

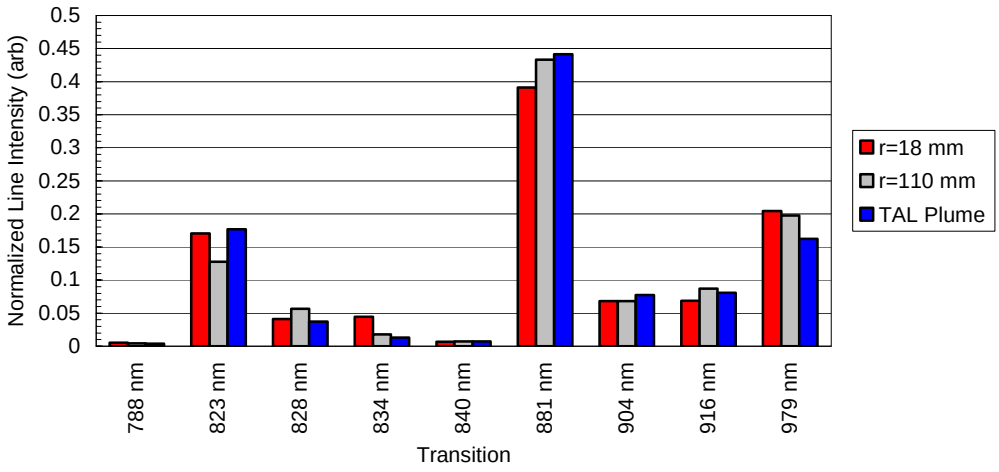

Figure 4. Normalized line intensity for the nine lines investigated. Two positions, inside the beam at *r* = 18 mm, and outside the beam at *r* = 110 mm, are shown. The data are compared to intensities acquired by Karabadzhak, et al. from the plume of a TAL thruster.

plume, is used as an estimate for the background signal. The line intensity for every peak of interested for every other position is reduced by the intensity of the corresponding peak at -130 mm.

C. Results and Discussion

Figure 4 shows sample normalized emission intensities—that is, the intensity of each line divided by the sum of all lines—for the nine lines investigated. It shows the values at two radial positions. In addition, the data are compared to the emissions measured by Karabadzhak, et al. in the plume of a TAL thruster. The intensities are comparable on every line except for the 834 nm line, which is off by 100% or more in the beam. This anomaly is seen across the entire beam. Karabadzhak and colleagues mention the possibility of interference on this line from an unidentified source. It is possible that our measurements exhibit more such interference.

Figure 5 shows the electron temperature as a function of position as determined by both the 3-line and the 9-line OES methods, as well as by Langmuir probe. All methods show a flat radial profile for the electron temperature, and thus agree qualitatively. For the OES methods, errors are determined from the covariance of the least squares fit of the modeled line intensities to the measured line intensities. The algorithm incorporates the 10% - 20% errors on the individual line intensities into its estimation of the best fit and the resulting error. Figure 5e shows the results of the Langmuir probe data, which confirms the even temperature distribution, and shows an electron temperature around 3.5 eV. The probe was not optimally sized to the plasma conditions, and the I-V traces were difficult to interpret. Errors in the Langmuir probe temperatures are estimated at 20%.

Figure 5a shows the electron temperature of the plasma as a function of radial position calculated using the 3-line method. Upon noting that the errors were relatively high at radial positions greater than 75 mm, we proposed that this region may be outside the beam of the HET. A model that does not include fast ion collisions would therefore better fit these data. For the 3-line analysis, removing the ion contribution reduces the KCD model to the standard coronal equilibrium model.[6] This model was applied, and its results are shown in Figure 5b. Since a large temperature error is indicative of a poor fit to the model, these results support our proposition. These data show that the beam radius was between 75 mm and 90 mm at the point of our measurements. Figure 5c shows the composite of the two methods, selecting only those points from each of the E_i = 300 eV and E_i = 0 model fits that exhibit good matches between model and experiment as judged by the small (less that 50%) errors. The point at 82 mm has been removed from this view since it shows relatively high errors in both models. It is reasonable to assume that because this point was at the boundary between the beam and the ambient plasma neither model fit well.

These results show that it may be possible to optically determine the divergence of the HET beam, which plays an important role in determining the overall thruster efficiency. If at a distance d from the exit plane of the thruster r_{max} is the distance from the thrust axis at which the model that best fits the data changes from one which includes ion-induced contributions to one that does not, then

a) 3-Line KCD Method (E_i = 300 eV)

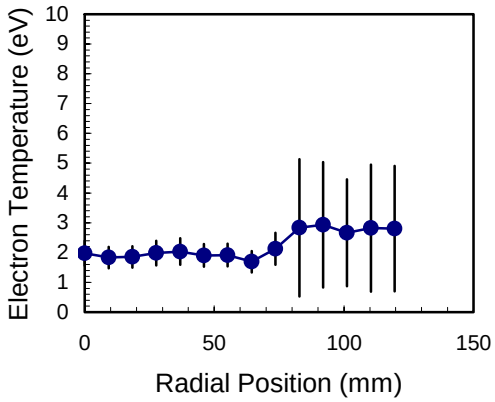

b) 3-Line Coronal Equilibrium Method (E_i = 0)

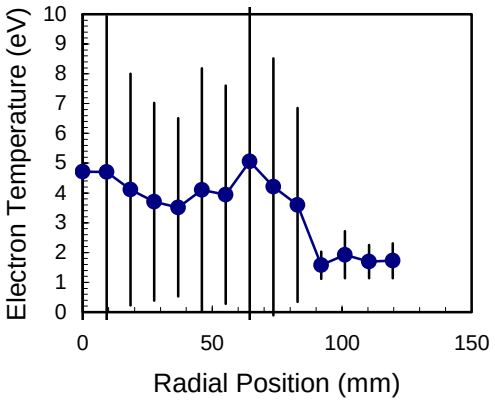

c) 3-Line KCD Method (Composite)

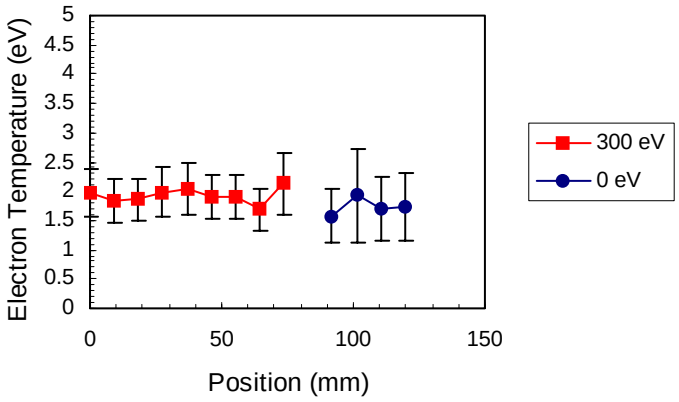

d) 9-Line KCD Method

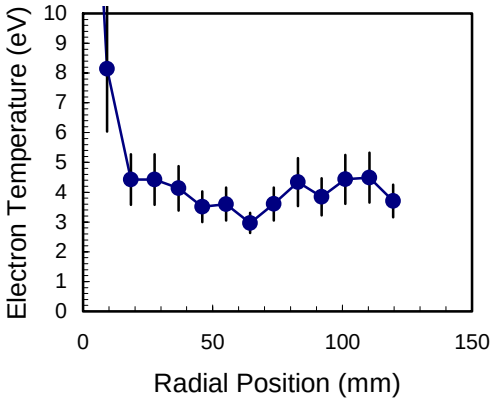

e) Langmuir Probe

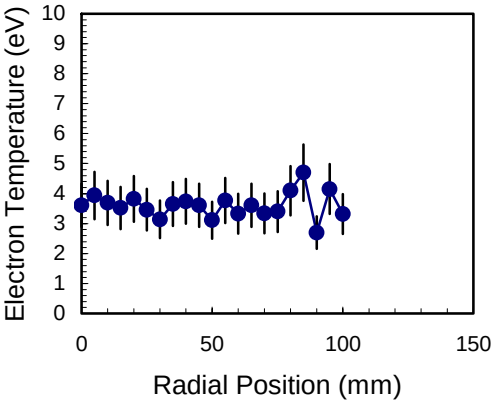

Figure 5. Electron temperature of the plume 160 mm downstream of the exit plane, as determined by a) OES using the 3-Line KCD model with fast ions, b) OES using the 3-Line coronal equilibrium model, c) OES composite, d) OES using the 9-Line KCD model, and e) Langmuir probe

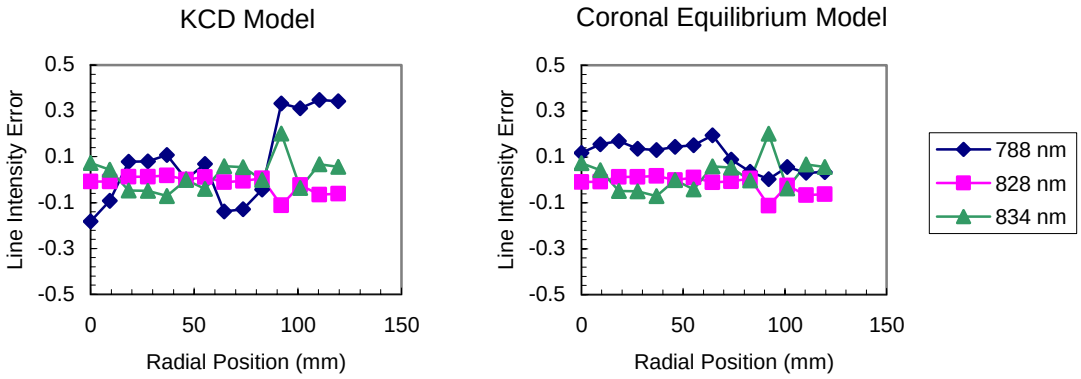

Figure 6. Fractional deviation of the modeled line intensity from the measured intensity for the 3-line KCD model (including fast ion contributions) and the coronal equilibrium model (excluding fast ion contributions)

$$\theta = \arctan\left(\frac{r_{max}}{d}\right) \tag{4}$$

where θ is the divergence half-angle. For this experiment, 75 mm < r_{max} < 90 mm and d = 160 mm, resulting in a divergence half-angle of between 25 and 30 degrees is calculated. Comparing this data to beam divergence values reported on the same thruster this half angle corresponds to the angle necessary to capture between 90 and 93 percent of the total beam current,[16] which suggests that the OES method compares well to the standard 90% divergence half angle measurement used with Faraday probe data.

Investigation into this phenomenon revealed that the 788 nm line is very sensitive to fast ions at the low electron temperatures exhibited here. Figure 6 shows the fractional deviation of the modeled line intensity from the measured line intensity for each of the three lines used in each analysis, both with and without fast ions. It shows that the 788 nm line is most affected by the inclusion of the ions. This is consistent with the cross section data of that line.[10,14]

Figure 5d shows the electron temperatures as determined by the best fit to the 9-line model that includes metastable contributions. The first two points at 0 and 10 mm are erroneous due to difficulties in the Abel inversion on certain lines. It is believed that these errors can be corrected with better alignment of the astigmatism-correcting optics. The temperature is approximately 2 eV hotter than that calculated by the 3-line model. This increase in temperature is consistent with observations by Karabadzhak and coworkers. It is believed to be a result of either line interference on the 834 nm line leading to erroneously high intensity measurements of that line or inaccuracies in the estimation of metastable cross sections used in the 9-line model. Most likely the error is some combination of both problems.

It should be noted that the 9-line OES measurements and the Langmuir measurements do show good agreement in absolute magnitude. However, the errors in the 9-line method are somewhat higher than those of the 3-line method in this experiment. These results were not expected, as the 3-line analysis is more likely to suffer from systematic errors due to the small signals and the potential interference on the 834 nm line. The most likely explanation for the difference in error is that exposure time normalization is inaccurate. The 3-line method used peaks which were all taken from the same segment of the spectra, that is, from one exposure. Thus, no errors were introduced through the exposure time normalization process used to mitigate the shutter time problems encountered in the experiment. The 9-line method requires peaks from multiple spectral segments and is thus subject to these errors.

III. Conclusion

We have applied the KCD model to the emissions from the plume of a laboratory HET similar to an Aerojet BPT-2000. Using a spectrographic imaging technique and the Abel inversion, we determined that the radial profile of the electron temperature at a distance of 160 mm downstream of the exit plane of the thruster is flat. The 9-line analysis agrees with the Langmuir probe data and shows that the temperature is between 3.5 and 4 eV. These

experiments agree with the work of Karabadzhak and colleagues in that the 3-line analysis underpredicts the electron temperature, as compared to the 9-line. However, Karabadzhak, et al. found the error in the 9-line analysis to be smaller than we report here. The combination of insufficient background suppression and exposure time uncertainty in our present experiment are the most likely sources of this discrepancy. Despite its low temperature, the 3-line analysis shows the sensitivity of the model to the presence of fast ions. These data suggest that the KCD model may be used as an optical method for determining beam divergence. It is expected that the 9-line technique will also exhibit this behavior once the errors due to the exposure time uncertainty are corrected.

Future work at Michigan Tech will eliminate the experimental problems encountered. First, exposure times below 10 ms cannot be used with the present equipment. In order to avoid saturating the detector we need either to introduce neutral density filters, or to decrease the sensitivity of the CCD, possibly by binning fewer pixels into image tracks.

Second, more data points need to be taken across the radius of the plume in order to better apply the Abel inversion. This may be accomplished in two ways. The optics may be adjusted so that we acquire only one half of the plume, rather than the entire diameter. This adjustment would double the number of available data points. In order to avoid interference from the cathode plume, the half of the thruster plume further from the cathode should be imaged. If the astigmatism correction of the spectrograph is improved, better focus may be achieved which would allow for a significant increase in the number of points, perhaps up to the maximum resolution of the CCD detector, 254 pixels. It is presently unknown whether this can be accomplished with the current equipment.

Third, no attempt was made to block reflections on the tank wall and other background objects. This is probably not a significant source of error near in the central regions of the plume, as the main signal appeared quite bright. However, towards the edges this may be more problematic. Since the Abel inversion tends to propagate errors in the radial edges towards the center, it is very important that this problem be addressed. The placement of a black surface behind the plume should be sufficient to prevent these reflections from entering the spectrograph.

After correcting the problems listed above, we intend to study a range of distances from the exit plane. Successful mapping of more varied plume regions will add confidence to the applicability of the model and its usefulness as a plasma diagnostic.

In addition to experimental improvements, improvements in the model also need to be addressed. Recently published metastable cross sections[17] should eliminate an approximation which is a potential source of error in the metastable model. A modified fit routine that incorporates these cross sections will be applied.

Acknowledgments

We would like to thank Dr. Rainer A. Dressler and Dr. Yu-Hui Chiu of the Air Force Research Laboratory at Hanscom Air Force Base, Massachusetts for their support in this project. They have been generous with both their equipment and their time, and without them this research would not have been possible. Further thanks go to Dr. George Karabadzhak of TsNIMASH, Moscow, Russia for his patient explanations and encouragement. This research has been supported by the Air Force Office of Scientific Research and the Air Force Space Scholars Program.

References

[1] Tverdokhlebov, S., Semenkin, S., Polk, J., "Bismuth propellant option for very high power TAL thruster," *40th AIAA Aerospace Sciences Meeting,* Paper No. AIAA-2002-0348, Reno, NV, 2002.

[2] Meezan, N. B., Hargus, J. W. A., Schmidt, D. P., and Cappelli, M. A., "Optical study of anomalous electron transport in a laboratory Hall thruster," AIAA-1999-2284, *35th AIAA/ASME/SAE/ASEE Joint Propulsion Conference and Exhibit,* Los Angeles, CA, June 20-24, 1999.

[3] Karabadzhak, G. F., Chiu, Y., Williams, S., and Dressler, R. A., "Hall thruster optical emission analysis based on single collision luminescence spectra," *37th AIAA/ASME/SAE/ASEE Joint Propulsion Conference and Exhibit*, AIAA-2001-3893, Salt Lake City, UT, July 8-11, 2001.

[4] Bugrova, A. I., et. al., "Spectral characteristics of closed drift Hall thuster radiation energy," *Teplophyzika Visokikj Temperatur*, Vol. 19, No. 2, 1981, p. 428

[5] Bugrova, A. I., Ermolenko, V. A., and Sokolov, A. S., "Optical investigation of neutral component of nonequilibrium xenon plasma," *Teplophyzika Visokikj Temperatur*, Vol. 25 No. 6, 1987, p. 1080.

[6] Hutchinson, I. H., *Principles of Plasma Diagnostics*, 2nd ed., Cambridge University Press, Cambridge, UK 2002, pp. 223-227.

[7] Karabadzhak, G. F., Semenkin, A.V., Tverdokhlebov, A. O., and Manzella, D. J., "Investigation of TAL optical emissions," *25th International Electric Propulsion Conference*, IEPC-97-131, Cleveland, OH, Aug. 24-28, 1997.

[8] Prioul, M., Roche, S., Pagnon, D., Magne, L., Touzeau, M., Bouchoule, A., and Lasgorceix, P., "Insight on closed electron drift thrusters obtained with a discharge shutter as diagnostic tool" *37th AIAA/ASME/SAE/ASEE Joint Propulsion Conference and Exhibit*, AIAA-2001-3893, Salt Lake City, UT, July 8-11, 2001.

[9] Karabadzhak, G. F., Chiu, Y., and Dressler, R. A., "Passive optical diagnostic of Xe propelled Hall thrusters. Part II," *Journal of Applied Physics*, Vol. 99, No. 113305 (online), 9 Jun. 2006.

[10] Chiu, Y., Austin, B. L., Williams, S., Dressler, R. A., Karabadzhak, G. F., "Passive optical diagnostic of Xe propelled Hall Thrusters. Part I," *Journal of Applied Physics*, Vol. 99, No. 113304 (online), 9 Jun. 2006.

[11] King, D., et. al., "Development of the BPT family of U.S.-designed Hall current thrusters for commercial LEO and GEO applications," AIAA-98-3338, *34th AIAA/ASME/SAE/ASEE Joint Propulsion Conference and Exhibit*, Cleveland, OH, July 13-15, 1998.

[12] Foreman, W. T., "Lens Correction of Astigmatism in a Czerny-Turner Spectrograph," *Applied Optics*, Vol. 7, No. 6, pp. 1053–1059, Jun. 1968.

[13] Mausbach, M., "Parameterization of the Laframboise theory for cylindrical Langmuir probe analysis," *Journal of Vacuum Science and Technology A*, Vol. 15, No. 6, Nov. 1997, pp. 2923-2929.

[14] Fons, J. T., and Lin, C. C. "Measurement of the cross sections for electron-impact excitation into the $5p^5 6p$ levels of xenon," *Physical Review A*, Vol. 58, No. 6, Dec. 1998, pp. 4603–4615.

[15] Deutsch, M., and Beniaminy, I., "Inversion of Abel's integral equation for experimental data," *Journal of Applied Physics*, Vol. 54, No. 1, Jan. 1983, pp. 137–143.

[16] Ross, J. L., Kieckhafer, A. W., and King, L. B., "Performance diagnostics for a low specific impulse thruster," AIAA-2006-4474, *42nd AIAA/ASME/SAE/ASEE Joint Propulsion Conference and Exhibit*, Sacramento, CA, Jul. 12-14, 2006.

[17] Jung, R. O., Boffard, J. B., Anderson, L. W., and Lin, C. C., "Electron-impact excitation cross sections from the xenon J = 2 metastable level," *Physical Review A*, Vol. 72, No. 022723 (online), Aug. 2005.